

## Producing and quantifying enriched *para*-H<sub>2</sub>

Brian A. Tom,<sup>1</sup> Siddhartha Bhasker,<sup>1,a)</sup> Yuki Miyamoto,<sup>2</sup> Takamasa Momose,<sup>2,b)</sup> and Benjamin J. McCall<sup>1,3,c)</sup>

<sup>1</sup>Department of Chemistry, University of Illinois at Urbana-Champaign, Urbana, Illinois 61801, USA

<sup>2</sup>Department of Chemistry, The University of British Columbia, Vancouver, British Columbia V6T 1Z1, Canada

<sup>3</sup>Department of Astronomy, University of Illinois at Urbana-Champaign, Urbana, Illinois 61801, USA

(Received 26 September 2008; accepted 29 December 2008; published online 30 January 2009)

The production of enriched *para*-H<sub>2</sub> is useful for many scientific applications, but the technology for producing and measuring *para*-H<sub>2</sub> is not yet widespread. In this note and in the accompanying auxiliary material, we describe the design, construction, and use of a versatile standalone converter that is capable of producing *para*-H<sub>2</sub> enrichments of up to  $\geq 99.99\%$  at continuous flow rates of up to 0.4 SLM. We also discuss *para*-H<sub>2</sub> storage and back conversion rates, and improvements to three techniques (thermal conductance, NMR, and solid hydrogen impurity spectroscopy) used to quantify the *para*-H<sub>2</sub> enrichment. © 2009 American Institute of Physics. [DOI: 10.1063/1.3072881]

There are many types of experiments that benefit from the use of a highly enriched or precisely controlled sample of *para*-H<sub>2</sub>. Examples include nuclear magnetic resonance techniques that exploit the signal-enhancing *para*-H<sub>2</sub> effect,<sup>1</sup> the production of solid hydrogen crystals for matrix isolation spectroscopy,<sup>2-5</sup> and superfluidity studies.<sup>6</sup> In addition, dissociative recombination experiments with astrochemical implications,<sup>7-10</sup> mass spectroscopic experiments to study deuterium fractionation in dense molecular clouds,<sup>11</sup> and fundamental chemical physics studies involving the spin modifications of hydrogenic species<sup>12-15</sup> receive continued attention.

The first device built to convert *ortho*-H<sub>2</sub> to *para*-H<sub>2</sub> used a tube filled with an activated charcoal catalyst.<sup>16</sup> The tube was immersed in a cryogen such as liquid nitrogen or liquid hydrogen (for higher *para* enrichments), and the backing pressure was set such that the H<sub>2</sub> was forced to flow through the catalyst.

A more convenient converter was developed by Tam and Fajardo<sup>17</sup> using a closed-cycle <sup>4</sup>He cryostat. This system merged automated control over a range of temperatures with the high enrichments accessible when using liquid helium as a cryogen. It was optimized to deposit solid *para*-H<sub>2</sub> for matrix isolation spectroscopy at a rate of  $\sim 0.12$  SLM (standard liters per minute). We have developed a new system that is conceptually similar to theirs but is a standalone system that can be readily adapted for many experiments. We have also tested our system to considerably higher flow rates, up to 0.4 SLM. In this note we highlight the unique design aspects of this converter, back conversion rates of stored *para*-H<sub>2</sub>, and improvements we have made to three enrichment measurement techniques. The auxiliary material<sup>18</sup> contains a detailed description of the design, fabrication, and use of the converter, along with a more detailed discussion of the enrichment measurement methods.

The *para*-H<sub>2</sub> converter consists of a locally modified commercial closed-cycle <sup>4</sup>He cryostat. Austenitic stainless steel tubing is used to route hydrogen gas into and out of a coiled reaction section mounted to the cold head. The coil is a solid piece of oxygen-free high conductivity copper (OFHC) around which 1/8 in. copper tubing has been wound (Fig. 1). The input to the coil reactor is at the top end of the device. The copper tubing winds downward around the OFHC and passes through the center adjacent to the cold head before attaching to the outgoing stainless steel tubing. The solid piece was machined with a single groove that winds continuously around the plug from top to bottom just above the base, allowing the copper tubing to be recessed and soldered into the OFHC. The coiled tubing, which makes approximately 14 loops around the OFHC core, provides approximately 1.3 m of path length. An alternative design (which we have also constructed) uses 1/4 in. copper tubing, allowing for higher throughput but shorter interaction length. The tubing is filled with a 30 × 50 mesh hydrous ferric oxide catalyst, which is contained by small disks cut from porous 60 mesh stainless steel filter material that have been crimped into the ends of the tube.

The converter can feed an experiment with a continuous flow of *para*-H<sub>2</sub> or fill a storage vessel for later use. The 1/4 in. diameter converter was routinely used to produce 99.99% enriched *para*-H<sub>2</sub> at a rate of 0.4 SLM, and the converter constructed with the smaller diameter tubing was tested at the same enrichment at rates of up to 0.34 SLM (higher flow rates have not been tested).

To minimize back conversion of stored *para*-H<sub>2</sub>, the prepared gas was kept in a Teflon-lined sample cylinder, the ends of which were sealed with a brass valve and end cap. The rate of back conversion in the sample cylinder was 1.7% per week (see Table I for other back conversion rates) and was most likely due to small sections of exposed stainless steel threading near the brass fittings. The back conversion rate increased when the system was contaminated with impurities, with the paramagnetic O<sub>2</sub> molecule the likely culprit. For this reason, the entire system was evacuated by a

<sup>a)</sup>Present address: Ernst and Young, Mumbai, India.

<sup>b)</sup>Electronic mail: momose@chem.ubc.ca.

<sup>c)</sup>Electronic mail: bjmcCall@illinois.edu.

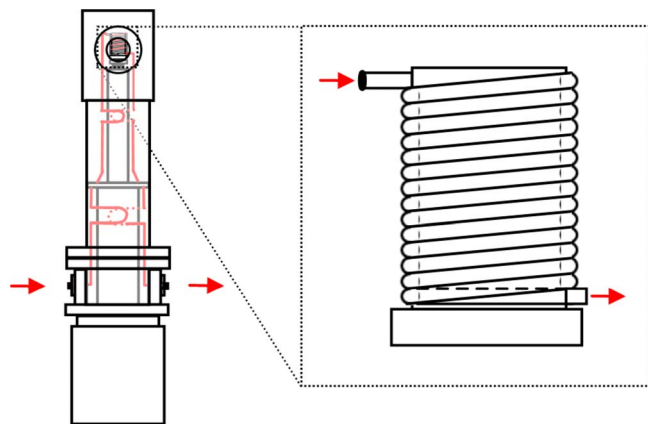


FIG. 1. (Color online) Left: An overview of the *para*-H<sub>2</sub> converter. Right: A closeup of the coil section where the catalytic conversion occurs. More details on the converter are given in the auxiliary material (Ref. 18).

turbomolecular pump for 24–48 h before a new sample of *para*-H<sub>2</sub> was produced. The high conversion rate observed in glass NMR tubes is also thought to be due to contamination by O<sub>2</sub>, from imperfect seals on the tubes and from incompletely degassed tetramethyl silane (TMS) (when used). We improved upon three methods used to measure *para*-H<sub>2</sub> enrichment: thermal conductance, nuclear magnetic resonance, and absorption spectroscopy in solid hydrogen. Our work on each of these techniques is described in detail in the auxiliary material,<sup>18</sup> and here we provide only brief descriptions.

The thermal conductance method takes advantage of the different thermal conductivities of *ortho*- and *para*-H<sub>2</sub> at low temperatures, measured using a thin filament through which a constant current is passed. The design of glass thermal conductance measurement cells is thoroughly discussed by Farkas<sup>19</sup> and Stewart and Squires.<sup>20</sup> Our cell is an improvement on their design because it is constructed from stainless steel flanges and nipples, providing easier access to the filament for maintenance and avoiding the need for glasswork. To take a measurement, the cell was suspended in a bath of liquid N<sub>2</sub> and 50 mbar of gas was introduced. Using a current source, 105 mA was applied to the wire and the required voltage was recorded. The cell was calibrated using samples of known *para*-H<sub>2</sub> enrichment, and the device had reproducibilities of  $\sim 0.7\%$  and  $\sim 0.8\%$  (in units of the percent enrichment) for low and high *para*-H<sub>2</sub> enrichments, respectively, based on measurements taken over a period of 6 months. Between these measurements the instrument would remain idle for extended periods of time, usually with a few millibars of internal pressure. Measurements obtained over a shorter time period usually fell within  $\sim 0.3\%$  for both the

TABLE I. The back conversion of *para*-H<sub>2</sub> in various storage vessels as measured by thermal conductance and NMR. In the first two entries, the starting enrichment was  $\sim 99.9\%$  *para*-H<sub>2</sub>. TMS is a NMR reference standard used in some of our enrichment measurements.

Type	<i>para</i> -H <sub>2</sub> back conversion
Stainless steel, <sup>a</sup> Teflon lined	(1.7% $\pm$ 0.4%)/week
Aluminum, <sup>a</sup> unlined	(1.9% $\pm$ 0.7%)/week
Glass NMR tube (with TMS)	(0.8% $\pm$ 0.1%)/h
Glass NMR tube (without TMS)	(0.4% $\pm$ 0.2%)/h

<sup>a</sup>With brass valve and fittings.

high and low enrichment regimes, which is comparable to the precision found by Assael *et al.*<sup>21</sup> using the transient hot wire method. The reason for this time dependence is not well understood.

Nuclear magnetic resonance is another method for measuring the enrichment of *para*-H<sub>2</sub> that is readily available to many laboratories, given the ubiquity of NMR spectrometers. The technique is based on the fact that *para*-H<sub>2</sub> (with a total nuclear spin of 0) has no NMR signal, whereas *ortho*-H<sub>2</sub> (spin 1) does. By comparing the NMR spectrum of a sample of unknown enrichment with that of a known sample (e.g., normal H<sub>2</sub> with *ortho*:*para*=3:1), one can directly infer the enrichment of the unknown sample because the integrated peak area is directly proportional to the number density.<sup>22</sup> We filled one gas NMR tube, fitted with a J. Young valve, with 20–40 psi (gauge) of test gas, and another with normal H<sub>2</sub> at the same pressure. Spectra were obtained as quickly as possible after sample preparation (to minimize back conversion, see Table I) using a commercial 500 MHz NMR spectrometer. Based on limited measurements, the NMR approach offers an accuracy of better than  $\sim 0.5\%$  for highly enriched ( $>95\%$ ) samples and  $\sim 2.5\%$  for less enriched samples.

Both the thermal conductance and NMR techniques are ideal for relatively simple and quick measurements of *para*-H<sub>2</sub> enrichment. The strength of the thermal conductance technique is in the ease of construction, but it requires extensive calibration. The advantage of the NMR technique is its availability and the fact that no external calibration is needed. Despite these strengths, the limitations in the accuracy and precision of these techniques may make them unsuitable for certain applications. To obtain measurements with high accuracy and precision, we used solid hydrogen spectroscopy.

The  $Q_1(1)$  ( $v=1 \leftarrow 0$ ,  $J=1 \leftarrow 1$ ) transition of *ortho*-H<sub>2</sub> in solid *para*-H<sub>2</sub> has been used<sup>23</sup> to estimate the *ortho*-H<sub>2</sub> concentration ( $\Omega$ ), but this requires the growth of relatively large crystals of precisely known dimensions. Another approach utilizes Fourier transform infrared absorption spectra of impurities in solid H<sub>2</sub>. Yoshioka and Anderson<sup>24</sup> reported that the spectra of CH<sub>3</sub>F-(*ortho*-H<sub>2</sub>)<sub>*m*</sub> clusters in solid *para*-H<sub>2</sub> show well-separated peaks; we have discovered that the relative peak intensities of these clusters can be used to estimate  $\Omega$ .

As shown in Fig. 2, the peak intensity of each cluster is found to obey the Poisson distribution,  $f(\lambda; m) = \lambda^m e^{-\lambda} / m!$ , where  $m$  is the number of *ortho*-H<sub>2</sub> molecules in the cluster and  $\lambda$  is an empirically fit parameter. Values of  $\lambda$  determined in our experiment are plotted, along with those inferred from the spectra of Yoshioka and Anderson,<sup>24</sup> in Fig. 3 as a function of *ortho*-H<sub>2</sub> concentration. It should be noted that the relationship between the parameter  $\lambda$  and the *ortho*-H<sub>2</sub> concentration is consistent between these two separately measured data sets, indicating the universality of this method for the estimation of *ortho*-H<sub>2</sub> concentrations.

The parameter  $\lambda$  should be proportional to the *ortho* concentration if the clustering between CH<sub>3</sub>F and *ortho*-H<sub>2</sub> is a random process. Unfortunately, this is not the case in solid *para*-H<sub>2</sub> where preferential formation of larger, more stable *ortho*-H<sub>2</sub> clusters takes place. As a result, the relation between  $\lambda$  and  $\Omega$  is not linear. In Fig. 3, we fit the parameter  $\lambda$

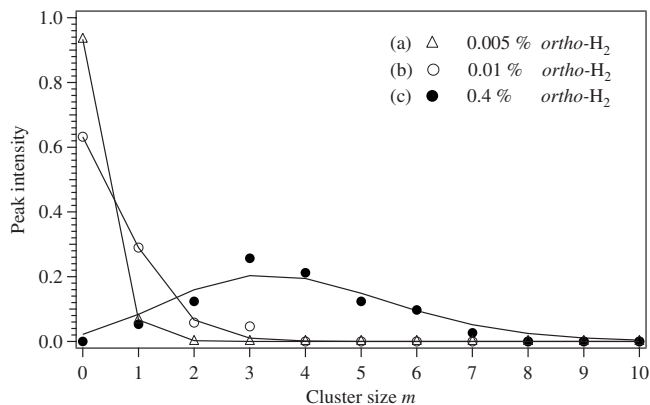


FIG. 2. The absorption peak intensities for each  $\text{CH}_3\text{F}-(ortho\text{-H}_2)_m$  cluster. The peak intensities are normalized so that the sum of all peaks is 1. Lines represent Poisson distributions (see text) with values of  $\lambda=(a)$  0.07, (b) 1.72, and (c) 3.82.

with the function  $\lambda=A[1-\exp(-B\Omega)]$ . The coefficients providing the best fit are  $A=10.0\pm 0.7$  and  $B=1.33\pm 0.18$ , with  $\Omega$  in units of percent. For *ortho* concentrations lower than 0.5%, one may use the simpler relation  $\lambda=10.2\ \Omega$ , as depicted by the broken line in Fig. 3. These relationships are purely empirical, but they provide fairly accurate estimates of the *ortho*- $\text{H}_2$  concentration when  $\Omega$  is lower than a few percent.

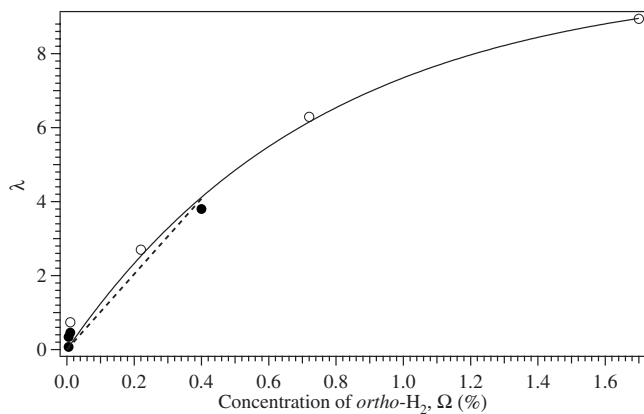


FIG. 3. Plot of the Poisson parameter  $\lambda$  as a function of *ortho*- $\text{H}_2$  concentration,  $\Omega$ , in units of %. The filled circles (●) are derived from data from the current experiment, and open circles (○) are derived from data of Yoshioka and Anderson (Ref. 24). The solid and broken lines represent empirical fits that can be used to determine  $\Omega$  from measured  $\lambda$  in unknown samples.

The University of Illinois team would like to acknowledge NSF Grant No. PHY 05-55486 for providing support for this project. Research at UBC was supported by a National Sciences and Engineering Research Discovery Grant in Canada and by the Japan Science and Technology Agency under the CREST project “Quantum Information Processing.”

<sup>1</sup>S. B. Duckett and C. J. Sleight, *Prog. Nucl. Magn. Reson. Spectrosc.* **34**, 71 (1999).

<sup>2</sup>T. Momose and T. Shida, *Bull. Chem. Soc. Jpn.* **71**, 1 (1998).

<sup>3</sup>L. Andrews and X. Wang, *Rev. Sci. Instrum.* **75**, 3039 (2004).

<sup>4</sup>M. E. Fajardo and S. Tam, *J. Chem. Phys.* **108**, 4237 (1998).

<sup>5</sup>Y.-P. Lee, Y.-J. Wu, and J. T. Hougen, *J. Chem. Phys.* **129**, 104502 (2008).

<sup>6</sup>A. C. Clark, X. Lin, and M. H. W. Chan, *Phys. Rev. Lett.* **97**, 245301 (2006).

<sup>7</sup>H. Kreckel, M. Motsch, J. Mikosch, J. Glosík, R. Plašil, S. Altevogt, V. Andrianarijaona, H. Buhr, J. Hoffmann, L. Lammich, M. Lestinsky, I. Nevo, S. Novotny, D. A. Orlov, H. B. Pedersen, F. Sprenger, A. S. Terekhov, J. Toker, R. Wester, D. Gerlich, D. Schwalm, A. Wolf, and D. Zajfman, *Phys. Rev. Lett.* **95**, 263201 (2005).

<sup>8</sup>H. Kreckel, A. Pettrignani, M. Berg, D. Bing, S. Reinhardt, S. Altevogt, H. Buhr, M. Froese, J. Hoffmann, B. Jordon-Thaden, C. Krantz, M. Lestinsky, M. Mendes, O. Novotný, S. Novotny, H. B. Pedersen, D. A. Orlov, J. Mikosch, R. Wester, R. Plašil, J. Glosík, D. Schwalm, D. Zajfman, and A. Wolf, *J. Phys.: Conf. Ser.* **88**, 012064 (2007).

<sup>9</sup>A. Pettrignani, H. Kreckel, M. H. Berg, S. Altevogt, D. Bing, H. Buhr, M. Froese, J. Hoffmann, B. Jordon-Thaden, C. Krantz, M. B. Mendes, O. Novotný, S. Novotny, D. A. Orlov, S. Reinhardt, and A. Wolf, arXiv:0810.0405v1.

<sup>10</sup>B. A. Tom, V. Zhaunerchyk, M. B. Wiczer, A. A. Mills, K. N. Crabtree, M. Kaminska, W. D. Geppert, M. Hamberg, M. af Ugglas, E. Vigren, W. J. van der Zande, M. Larsson, R. D. Thomas, and B. J. McCall, *J. Chem. Phys.* **130**, 031101 (2009).

<sup>11</sup>D. Gerlich, E. Herbst, and E. Roueff, *Planet. Space Sci.* **50**, 1275 (2002).

<sup>12</sup>M. Cordonnier, D. Uy, R. M. Dickson, K. E. Kerr, Y. Zhang, and T. Oka, *J. Chem. Phys.* **113**, 3181 (2000).

<sup>13</sup>D. Gerlich, *J. Chem. Phys.* **92**, 2377 (1990).

<sup>14</sup>D. Uy, M. Cordonnier, and T. Oka, *Phys. Rev. Lett.* **78**, 3844 (1997).

<sup>15</sup>J. P. Darr, A. C. Crowther, R. A. Loomis, S. E. Ray, and A. B. McCoy, *J. Phys. Chem. A* **111**, 13387 (2007).

<sup>16</sup>K. F. Bonhoeffer and P. Harteck, *Z. Phys. Chem.* **B4**, 113 (1929).

<sup>17</sup>S. Tam and M. Fajardo, *Rev. Sci. Instrum.* **70**, 1926 (1999).

<sup>18</sup>See EPAPS Document No. E-RSINAK-80-007902 for more detailed information about the *para*-hydrogen converter and the thermal conductance, NMR, and solid hydrogen measurement techniques. For more information on EPAPS, see <http://www.aip.org/pubservs/epaps.html>.

<sup>19</sup>A. Farkas, *Orthohydrogen, Parahydrogen, and Heavy Hydrogen* (Cambridge University Press, Cambridge, 1935), p. 20.

<sup>20</sup>A. T. Stewart and G. L. Squires, *J. Sci. Instrum.* **32**, 26 (1955).

<sup>21</sup>M. J. Assael, M. Dix, A. Lucas, and W. A. Wakeham, *J. Chem. Soc., Faraday Trans. 1* **77**, 439 (1981).

<sup>22</sup>C. Szítay, Jr., *TrAC, Trends Anal. Chem.* **11**, 332 (1992).

<sup>23</sup>D. P. Weliky, K. E. Kerr, T. J. Byers, Y. Zhang, T. Momose, and T. Oka, *J. Chem. Phys.* **105**, 4461 (1996).

<sup>24</sup>K. Yoshioka and D. T. Anderson, *J. Chem. Phys.* **119**, 4731 (2003).